

## BORIDING KINETICS OF Fe<sub>2</sub>B LAYERS FORMED ON AISI 1045 STEEL

J. Zuno-Silva<sup>a</sup>, M. Ortiz-Domínguez<sup>a</sup>, M. Keddam<sup>b\*</sup>, M. Elias-Espinosa<sup>c</sup>,  
O. Damián-Mejía<sup>d</sup>, E. Cardoso-Legorreta<sup>e</sup>, M. Abreu-Quijano<sup>a</sup>

<sup>a</sup> Universidad Autónoma del Estado de Hidalgo, Campus Sahagún, Sahagún-Otumba s/n, Hidalgo, México

<sup>b</sup> USTHB, Faculté de Génie Mécanique et Génie des Procédés, Lab. Techno. Matéri., El-Alia, Algeria

<sup>c</sup> Instituto Tecnológico y de Estudios Superiores de Monterrey-ITESM Campus Santa Fe, Obregón, México

<sup>d</sup> Universidad Nacional Autónoma de México-UNAM, Instituto de Investigación en Materiales, Circuito Exterior, s/n Ciudad Universitaria, Coyoacán, México

<sup>e</sup> Universidad Autónoma del Estado de Hidalgo, Centro de Investigaciones en Materiales y Metalurgia, Ciudad Universitaria Pachuca-Tulancingo, Hidalgo, México

(Received 23 March 2014; accepted 19 June 2014)

### Abstract

In the present work, a diffusion model was suggested to study the growth kinetics of Fe<sub>2</sub>B layers grown on the AISI 1045 steel by the pack-boriding treatment. The generated boride layers were analyzed by optical microscopy and X-ray diffraction analysis. The applied diffusion model is based on the principle of mass conservation at the (Fe<sub>2</sub>B/ substrate) interface. It was used to estimate the boron diffusion coefficients of Fe<sub>2</sub>B in the temperature range of 1123-1273 K. A validation of the model was also made by comparing the experimental Fe<sub>2</sub>B layer thickness obtained at 1253 K for 5 h of treatment with the predicted value. Basing on our experimental results, the boron activation energy was estimated as 180 kJ mol<sup>-1</sup> for the AISI 1045 steel.

Keywords: Boriding; Incubation time; Iron boride; Diffusion model; Growth kinetics; Activation energy.

### 1. Introduction

Boriding is a thermochemical treatment that modifies the surface of ferrous and non ferrous alloys by the thermodiffusion of boron atoms from a boriding agent [1]. It takes place at temperatures between 800 and 1000°C over a period of 1 to 10 h. As a consequence, the surface properties of treated materials such as hardness, corrosion resistance and wear resistance are improved. In practice, the most frequently used method is pack-boriding owing to its technical advantages [2]. In the powder-pack boriding, the pack contains a boron source such as a B<sub>4</sub>C compound, an activator to deposit atomic boron at the sample's surface and a diluent. The boriding of steels results in the formation of either one iron boride (Fe<sub>2</sub>B) or two iron borides (FeB and Fe<sub>2</sub>B) according to the boriding conditions. The modeling of the boriding kinetics is considered as a suitable tool to select the boride layer thickness according to the practical utilization of the borided material. In the case of the growth kinetics of Fe<sub>2</sub>B layers formed on different substrates [3-14], several diffusion models were published in the literature.

In the present study, an original diffusion model, based on solving the mass balance equation at the (Fe<sub>2</sub>B/ substrate) interface, was suggested to evaluate the boron diffusion coefficients through the Fe<sub>2</sub>B layers grown on AISI 1045 steel. The obtained Fe<sub>2</sub>B layers on AISI 1045 steel were characterized by optical microscopy and X-ray diffraction analysis. Basing on our experimental results, the boron activation energy was also evaluated when pack-boriding the AISI 1045 steel in the temperature range of 1123-1273 K.

### 2. The diffusion model

The model analyzes the growth of Fe<sub>2</sub>B layer on a saturated substrate with boron atoms as schematically shown in Figure 1. The  $f(x,t)$  function describes the boron distribution within the substrate before the nucleation of Fe<sub>2</sub>B phase.  $t_0^{Fe_2B}$  corresponds to the incubation time required to form the Fe<sub>2</sub>B phase when the matrix reaches a saturation state with boron atoms.  $C_{up}^{Fe_2B}$  represents the upper limit of boron content in Fe<sub>2</sub>B ( $= 60 \times 10^3 \text{ mol m}^{-3}$ ) while  $C_{low}^{Fe_2B}$  is the lower limit of boron content in Fe<sub>2</sub>B ( $= 59.8 \times 10^3 \text{ mol m}^{-3}$ )

\* Corresponding author: keddam@yahoo.fr

and the point  $x(t=t) = v$  refers to the  $\text{Fe}_2\text{B}$  layer thickness [15, 16]. The term  $C_{\text{ads}}^{\text{B}}$  is the effective adsorbed boron concentration during the boriding process [17]. From Figure 1,  $a_1 = C_{\text{up}}^{\text{Fe}_2\text{B}} - C_{\text{low}}^{\text{Fe}_2\text{B}}$  defines the homogeneity range of the  $\text{Fe}_2\text{B}$  layer,  $a_2 = C_{\text{low}}^{\text{Fe}_2\text{B}} - C_0$  is the miscibility gap and  $C_0$  is the boron solubility in the substrate. The diffusion zone underneath the  $\text{Fe}_2\text{B}$  layer can be ignored by setting ( $C_0 \approx 0 \text{ mol m}^{-3}$ ) [18, 19].

The following assumptions are taken into consideration during the formulation of the diffusion model:

- The growth kinetics is controlled by the boron diffusion in the  $\text{Fe}_2\text{B}$  layer.
- The  $\text{Fe}_2\text{B}$  phase nucleates after a certain incubation time.
- The boride layer grows because of the boron diffusion perpendicular to the specimen surface.
- Boron concentrations remain constant in the boride layer during the treatment.
- The influence of the alloying elements on the growth kinetics of the layer is not taken into account.
- The boride layer is thin compared to the sample thickness.
- A uniform temperature is assumed throughout the sample.
- Planar morphology is assumed for the phase interface.

The initial and boundary conditions for the diffusion problem are given by:

$$t = 0, x > 0, \text{ with: } C_{\text{Fe}_2\text{B}}[x(t), t = 0] = C_0 \approx 0. \quad (1)$$

Boundary conditions:

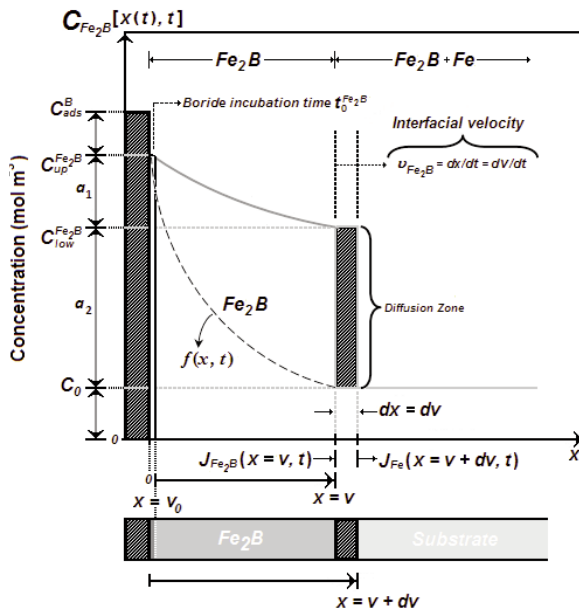


Figure 1. A schematic boron- concentration profile through the  $\text{Fe}_2\text{B}$  layer.

$$\left. \begin{aligned} C_{\text{Fe}_2\text{B}}[x(t=t_0^{\text{Fe}_2\text{B}}) = v_0, t = t_0^{\text{Fe}_2\text{B}}] &= C_{\text{up}}^{\text{Fe}_2\text{B}} \\ \text{(the upper boron concentration is kept constant)}, & \\ \text{for } C_{\text{ads}}^{\text{B}} > 60 \times 10^3 \text{ mol m}^{-3}, & \end{aligned} \right\} (2)$$

$$\left. \begin{aligned} C_{\text{Fe}_2\text{B}}[x(t=t) = v, t = t] &= C_{\text{low}}^{\text{Fe}_2\text{B}} \\ \text{(the boron concentration at the interface is} & \\ \text{kept constant)}, & \\ C_{\text{ads}}^{\text{B}} < 59.8 \times 10^3 \text{ mol m}^{-3} & \end{aligned} \right\} (3)$$

$v_0$  is a thin layer with a thickness of  $\approx 5 \text{ nm}$  that formed during the nucleation stage [20]. Thus  $v_0 (\approx 0)$  when compared to the thickness of  $\text{Fe}_2\text{B}$  layer ( $v$ ). The mass balance equation at the ( $\text{Fe}_2\text{B}$ /substrate) interface is expressed by Eq. (4):

$$\left( \frac{C_{\text{up}}^{\text{Fe}_2\text{B}} + C_{\text{low}}^{\text{Fe}_2\text{B}} - 2C_0}{2} \right) (A \cdot dv) = J_{\text{Fe}_2\text{B}}(x = v, t = t) \cdot (A \cdot dt) - J_{\text{Fe}}(x = v + dv, t = t)(A \cdot dt) \quad (4)$$

where  $A (= 1 \cdot 1)$  is defined as the unit area and  $C_0$  represents the boron concentration in the matrix. The flux  $J_{\text{Fe}_2\text{B}}$  and  $J_{\text{Fe}}$  are obtained from the Fick's First law as:

$$J_{\text{Fe}_2\text{B}}[x(t=t) = v, t = t] = - \{ D_{\text{Fe}_2\text{B}} \partial C_{\text{Fe}_2\text{B}}[x(t=t) = v, t = t] / \partial x \}_{x=v} \quad (5)$$

and

$$J_{\text{Fe}}[x(t=t) = v + dv, t = t] = - \{ D_{\text{Fe}} \partial C_{\text{Fe}}[x(t=t) = v + dv, t = t] / \partial x \}_{x=v+dv} \quad (6)$$

The term  $J_{\text{Fe}}$  is null since the boron solubility in the matrix is very low ( $\approx 0 \text{ mol m}^{-3}$ ) [18, 19].

Thus, Eq. (4) can be rewritten as:

$$\left( \frac{C_{\text{up}}^{\text{Fe}_2\text{B}} + C_{\text{low}}^{\text{Fe}_2\text{B}} - 2C_0}{2} \right) \frac{dx(t)}{dt} \Big|_{x(t)=v} = - D_{\text{Fe}_2\text{B}} \frac{\partial C_{\text{Fe}_2\text{B}}[x(t), t = t]}{\partial x} \Big|_{x(t)=v} \quad (7)$$

The diffusion of atomic boron in the substrate is governed by the Fick's Second law given by:

$$\frac{\partial C_{\text{Fe}_2\text{B}}[x(t), t]}{\partial t} = D_{\text{Fe}_2\text{B}} \frac{\partial^2 C_{\text{Fe}_2\text{B}}[x(t), t]}{\partial x^2} \quad (8)$$

By solving Eq. (8), and applying the boundary conditions proposed in Eqs.(2) and (3), the solution of Eq.(8) is expressed by Eq. (9) if the boron diffusion coefficient in  $\text{Fe}_2\text{B}$  is constant for a given boriding temperature :

$$C_{\text{Fe}_2\text{B}}[x(t), t] = C_{\text{up}}^{\text{Fe}_2\text{B}} + \frac{C_{\text{low}}^{\text{Fe}_2\text{B}} - C_{\text{up}}^{\text{Fe}_2\text{B}}}{\text{erf}\left(\frac{v}{2\sqrt{D_{\text{Fe}_2\text{B}}t}}\right)} \text{erf}\left(\frac{x}{2\sqrt{D_{\text{Fe}_2\text{B}}t}}\right) \quad (9)$$

By substituting the derivative of Eq. (9) with respect to the distance  $x(t)$  into Eq. (7), Eq. (10) is obtained:

$$\left( \frac{C_{up}^{Fe_2B} + C_{low}^{Fe_2B} - 2C_0}{2} \right) \frac{dv}{dt} = \sqrt{\frac{D_{Fe_2B}}{\pi t}} \frac{C_{up}^{Fe_2B} - C_{low}^{Fe_2B}}{\operatorname{erf}\left(\frac{v}{2\sqrt{D_{Fe_2B}t}}\right)} \exp\left(-\frac{v^2}{4D_{Fe_2B}t}\right) \quad (10)$$

$0 \leq x \leq v$  for .

The parabolic growth law for the  $Fe_2B$  layer is expressed by:

$$v = 2\varepsilon D_{Fe_2B}^{1/2} t^{1/2} \quad (11)$$

Substituting the derivative of Eq.(11) with respect to the time into Eq. (10), Eq. (12) is deduced:

$$\left( \frac{C_{up}^{Fe_2B} + C_{low}^{Fe_2B} - 2C_0}{2} \right) \varepsilon = \sqrt{\frac{1}{\pi}} \frac{C_{up}^{Fe_2B} - C_{low}^{Fe_2B}}{\operatorname{erf}(\varepsilon)} \exp(-\varepsilon^2) \quad (12)$$

The normalized growth parameter ( $\varepsilon$ ) for the ( $Fe_2B$ /substrate) interface can be estimated numerically by the Newton-Raphson method [21]. It is assumed that expressions  $C_{up}^{Fe_2B}$ ,  $C_{low}^{Fe_2B}$  and  $C_0$ , do not depend significantly on temperature (in the considered temperature range) [16].

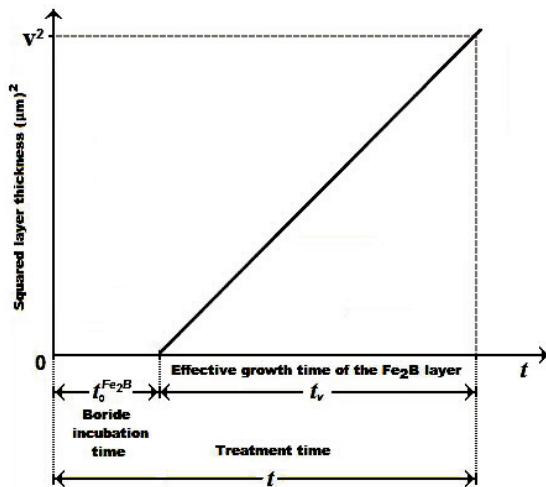


Figure 2. A Schematic representation of the square of the layer thickness as a function of treatment time.

A schematic representation of the square of the layer thickness against linear time ( $v^2 = 4\varepsilon^2 D_{Fe_2B} t = 4\varepsilon^2 D_{Fe_2B} (t_v + t_0^{Fe_2B})$ ) is depicted in Figure 2.  $t_v (= t - t_0^{Fe_2B})$  is the effective growth time of the  $Fe_2B$  layer and  $t$  is the treatment time.

### 3. Experimental procedure

#### 3.1 The boriding process

The material to be borided is AISI 1045 steel. It has a nominal chemical composition of 0.43–0.50% C, 0.15–0.30% Si, 0.60–0.90% Mn, 0.040% P, 0.050% S. The samples have a cubic shape with dimensions of 10 mm x 10 mm x 10 mm x. Prior to the boriding process, the specimens were polished, ultrasonically cleaned in an alcohol solution and deionized water for 15 min at room temperature, and dried and stored under clean-room conditions. The samples were packed along with a Durborid fresh powder mixture in a closed cylindrical case (AISI 304L). The used powder mixture has an average size of 30  $\mu\text{m}$ . The powder-pack boriding process was carried out in a conventional furnace under a pure argon atmosphere in the temperature range of 1123 - 1273 K. Four treatment times (2, 4, 6 and 8 h) were selected for each temperature. After the completion of boriding treatment, the container was removed from the furnace and slowly cooled to room temperature.

#### 3.2 Experimental techniques

The borided samples were cross-sectioned for metallographic examinations using a LECO VC-50 cutting precision machine. The cross-sectional morphology of the boride layers was observed with the Olympus GX51 optical microscope in a clear field. The boride layer thickness was automatically measured with the aid of MSQ PLUS software. To ensure the reproducibility of the measured layers thicknesses, fifty measurements were collected in different sections of the borided AISI 1045 steel samples to estimate the  $Fe_2B$  layer thickness; defined as an average value of the long boride teeth [22–24]. The phases present in the boride layers were investigated by an X-Ray Diffraction (XRD) equipment (Equinox 2000) using  $CoK_{\alpha}$  radiation of 0.179 nm wavelength.

### 4. Results

#### 4.1 OM observations of the borided layers

Figure 3 shows the optical micrographs of the cross-section of boride layers formed on AISI 1045 steel at 1173 K for different treatment times (2, 4, 6 and 8 h).

#### 4.2 XRD analysis

Figure 4 gives the XRD pattern obtained at the surface of borided AISI 1045 steel at 1273 K for 8 h of treatment. It indicates the formation of  $Fe_2B$  phase showing a difference in the diffracted intensities due to its anisotropic nature.

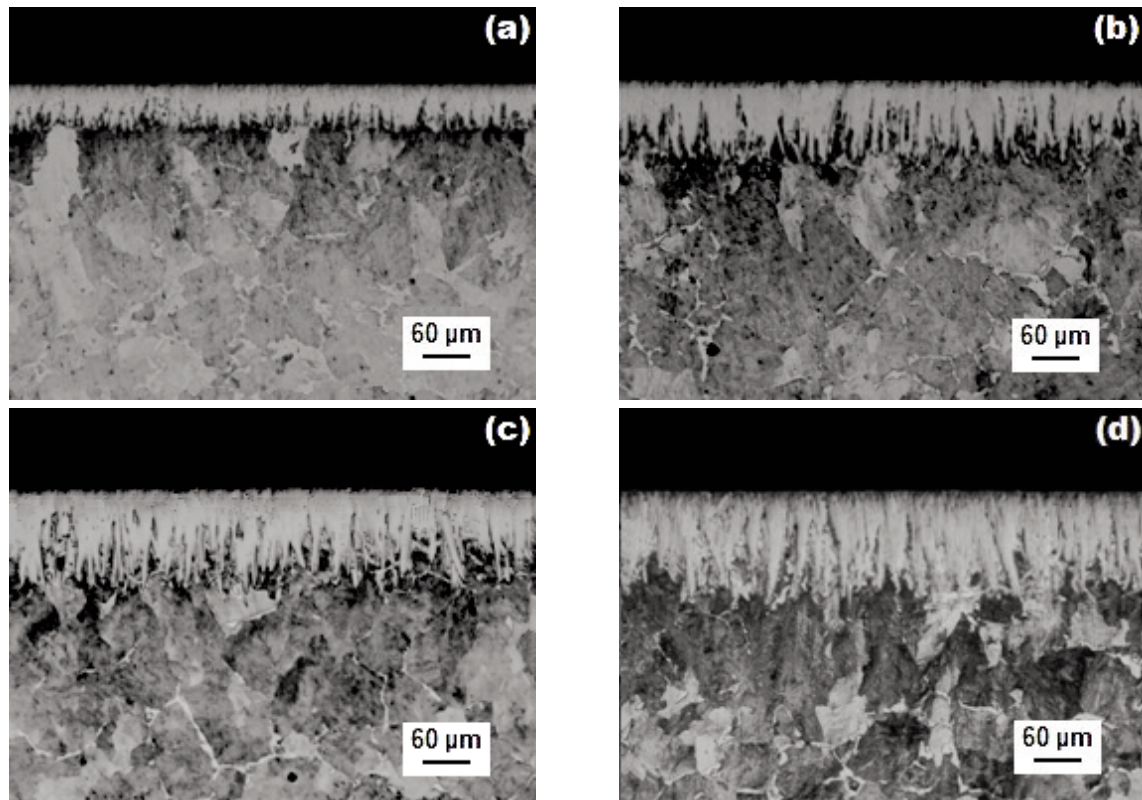


Figure 3. Optical micrographs of the boride layers formed at the surface of AISI 1045 steel treated at 1173 K during a variable time: (a) 2 h, (b) 4 h, (c) 6 h and (d) 8 h.

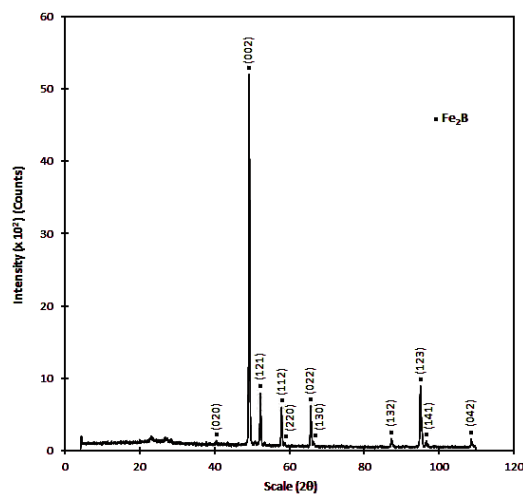


Figure 4. XRD pattern obtained at the surface of the borided AISI 1045 steel treated at 1273 K for 8 h.

#### 4.3 Estimation of boron activation energy

The kinetic study of  $\text{Fe}_2\text{B}$  layers formed on the AISI 1045 steel is necessary to estimate the boron diffusion coefficients of  $\text{Fe}_2\text{B}$  layers using the present model. Figure 5 describes the evolution of the squared value of  $\text{Fe}_2\text{B}$  layer thickness as a function of time for

different temperatures where the slopes of the linear curves provide the values of growth constants ( $= 4\varepsilon^2 D_{\text{Fe}_2\text{B}}$ ). Table 1 summarizes the estimated value of boron diffusion coefficient in  $\text{Fe}_2\text{B}$  at each temperature along with the squared normalized value of  $\varepsilon$  parameter determined from Eq. (12).

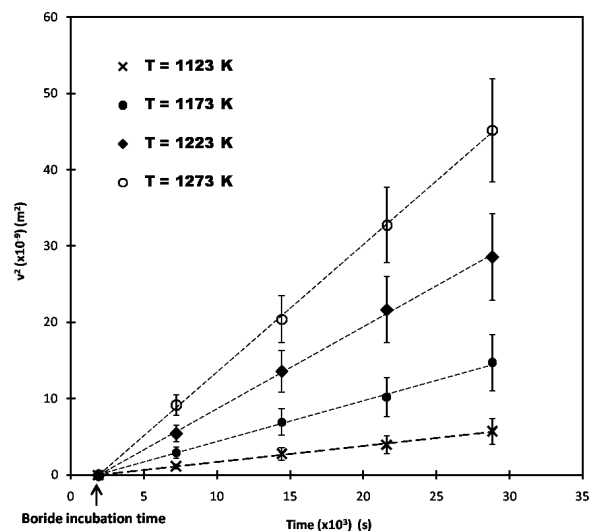


Figure 5. The square of  $\text{Fe}_2\text{B}$  layers thickness dependence of the temperature and time.

**Table 1.** The squared value of normalized growth parameter and boron diffusion coefficients in Fe<sub>2</sub>B as a function of the boriding temperature.

Temperature (K)	Type of layer	$\varepsilon^2$ (Dimensionless)	$4\varepsilon^2 D_{Fe_2B}$ ( $\mu\text{m}^2\text{s}^{-1}$ )
1123	Fe <sub>2</sub> B	1.747141 x 10 <sup>-3</sup>	1.79 x 10 <sup>-1</sup>
1173			5.00 x 10 <sup>-1</sup>
1223			11.0 x 10 <sup>-1</sup>
1273			17.0 x 10 <sup>-1</sup>

To get the value of boron activation energy for the AISI 1045 steel, it is necessary to plot the natural logarithm of boron diffusion coefficient in Fe<sub>2</sub>B versus the reciprocal temperature according to the Arrhenius equation. Figure 6 shows the temperature dependence of boron diffusion coefficient through the Fe<sub>2</sub>B layers where the slope of the straight line represents the value of boron activation energy (= 180 kJ mol<sup>-1</sup>) using a linear fitting with a correlation factor equal to 0.9813. The temperature dependence of  $D_{Fe_2B}$  is given by Eq.(13) as follows:

$$D_{Fe_2B} = 7.0 \times 10^{-3} \exp(-180 \text{ kJmol}^{-1} / RT), \quad (13)$$

where:  $R = 8.314 \text{ J mol}^{-1} \text{ K}^{-1}$  and T the temperature in Kelvin.

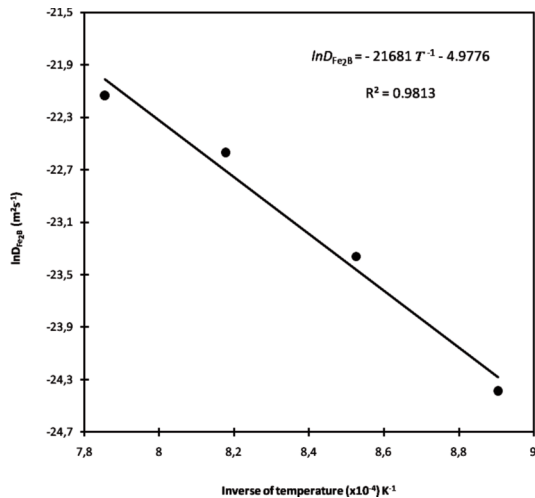


**Figure 6.** The boron diffusion coefficients in the Fe<sub>2</sub>B phase dependence of the temperature.

Table 2 shows a comparison of the boron activation energies in case of some borided steels [25, 30]. The estimated value of boron activation energy (= 180 kJ mol<sup>-1</sup>) for the AISI 1045 steel is very close to that obtained in the reference work [30] but different from other values [25,28]. This difference is due to the choice of the boriding method and to the effect of chemical composition of the substrate.

The present model was validated by comparing the experimental value of Fe<sub>2</sub>B layer thickness with

the predicted value at 1253 K for 5 h using Eq. (14):

$$v = 2\varepsilon D_{Fe_2B}^{1/2} t^{1/2} = \sqrt{17 D_{Fe_2B} t / 2500} \quad (14)$$

**Table 2.** A comparison of the boron activation energies for some borided steels using different boriding methods.

Material	Boriding method	Boron activation energy (kJ mol <sup>-1</sup> )	Ref
SAE 1035	Salt-bath	227.51	[25]
Low carbon steel	Electrochemical	175.51	[26]
AISI 1018	Electrochemical	172.75 ±8.6	[27]
Mild steel	SPS	145.84	[28]
AISI 1018	Paste	153	[29]
AISI 1045	Paste	179	[30]
AISI 1045	Powder	180	Present study

Figure 7 shows the optical micrograph of the cross-section of boride layer formed at 1253 K for 5 h.

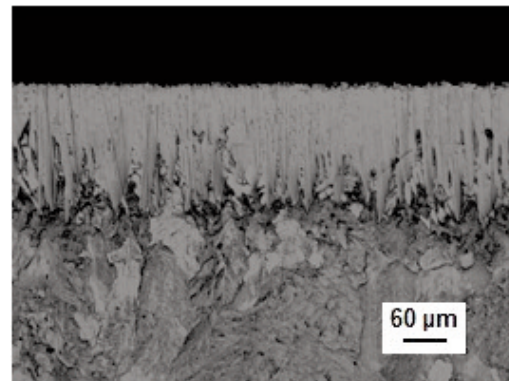


**Figure 7.** Optical micrograph of the cross-section of Fe<sub>2</sub>B layer formed on AISI 1045 steel during the powder-pack boriding at 1253 K for 5 h.

Table 3 gives a comparison between the experimental value of Fe<sub>2</sub>B layer thickness and the predicted one using Eq. (14). A good agreement was then obtained between the experimental value of Fe<sub>2</sub>B layer thickness and the predicted one for the borided AISI 1045 steel at 1253 K for 5 h.

**Table 3.** Predicted and estimated values of the Fe<sub>2</sub>B layer thickness obtained at 1253 K for a treatment time of 5 h.

Temperature (K)	Type of layer	Boride layer thickness (mm) estimated by Eq. (14)	Experimental boride layer thickness (mm)
1253	Fe <sub>2</sub> B	174.26	167.84±14.29

## 5. Discussions

The AISI 1045 steel was pack-borided in the temperature range of 1123–1273 K for studying the kinetics of formation of Fe<sub>2</sub>B layers. The XRD analysis confirmed the presence of Fe<sub>2</sub>B phase with a difference in the diffracted intensities due to its anisotropic nature [22]. The OM observations revealed the formation of Fe<sub>2</sub>B layers with a saw-tooth morphology. This particular morphology is observed in the boride layers formed on low-carbon steels [25-30] and Armco iron [4, 12, 15, 16] due to the absence of alloying elements in the substrate.

From Figure 3, it is seen that the Fe<sub>2</sub>B layer thickness increased with an increase in the boriding time because the boriding kinetics is a thermally activated phenomenon. In a kinetic point of view, the present model was applied to estimate the boron diffusion coefficient in Fe<sub>2</sub>B using Eq.(11). The boron activation energy of the AISI 1045 steel was estimated as 180 kJ mol<sup>-1</sup>. This value was compared with the data reported in the literature. The values of boron activation energies displayed in Table 2 depended on the boriding method, the chemical composition of the substrate and the mechanism of boron diffusion. The present model was also validated by comparing the experimental Fe<sub>2</sub>B layer thickness obtained at 1253 K for 5 h of treatment with the predicted value. The experimental value of Fe<sub>2</sub>B layer thickness agrees with the predicted value for the borided AISI 1045 steel at 1253 K for 5 h of treatment. The present model can be extended to the bilayer configuration (Fe<sub>2</sub>B + FeB) to study the boriding kinetics for any borided steel.

## 6. Conclusions

The AISI 1045 steel was pack-borided in the temperature range of 1123-1273 K for a period ranging from 2 to 8 h. The Fe<sub>2</sub>B layers were formed on the surface of AISI 1045 steel. A diffusion model was developed to estimate the boron diffusion coefficient of Fe<sub>2</sub>B at each boriding temperature. The validity of the present model was made by comparing the experimental Fe<sub>2</sub>B layer thickness obtained at 1253 K for 5 h of treatment with the predicted value. A good concordance was then observed between this experimental result and the predicted value by the model.

Finally, the boron activation energy of the AISI 1045 steel was estimated as 180 kJ mol<sup>-1</sup>. This value was compared with the data reported in the literature.

## Acknowledgements

*The work described in this paper was supported by a grant of CONACyT and PROMEP México. Also,*

*the authors want to thank to Ing. Martín Ortiz Granillo, who is in charge as Director of the Escuela Superior de Ciudad Sahagún which belongs to the Universidad Autónoma del Estado de Hidalgo, México, for all the facilities to accomplish this research work.*

## References

- [1] A. K. Sinha, J. Heat Treatment, 4 (1991) 437-447.
- [2] C. Meric, S. Sahin and S. S. Yilmaz, Mater. Res. Bull., 35 (2000) 2165-2172.
- [3] D. S. Kukharev, S. P. Fizenko, S. I. Shabunya, J. Eng. Phys. Therm., 69 (1996) 187-193
- [4] I. Campos, J. Oseguera, U. Figueroa, J. A. Garcia, O. Bautista, G. Keleminis, Mater. Sci. Eng. A 352 (2003) 261-265.
- [5] M. Keddad, Appl. Surf. Sci., 236 (2004) 451-455.
- [6] I. Campos-Silva, M. Ortiz-Domínguez, C. VillaVelazquez, R. Escobar, N. López, Defect Diffusion Forum, 272 (2007) 79-86.
- [7] R. D. Ramdan, T. Takaki, Y. Tomita, Mater. Trans., 49 (2008) 2625-2631.
- [8] M. Keddad, M. Ortiz-Domínguez, I. Campos-Silva, J. Martinez-Trinidad, Appl. Surf. Sci., 256 (2010) 3128-3132
- [9] M. Ortiz-Domínguez, E. Hernandez-Sanchez, J. Martinez-Trinidad, M. Keddad, I. Campos-Silva, Kovove Mater. 48 (2010) 1-6
- [10] I. Campos-Silva, N. López-Perrusquia, M. Ortiz-Domínguez, U. Figueroa-López, O. A. Gómez-Vargas, A. Meneses-Amador, G. Rodríguez-Castro, Kovove Mater. 47 (2009) 75-81.
- [11] M. Keddad, R. Chegroune, Appl. Surf. Sci., 256 (2010) 5025-5030
- [12] I. Campos-Silva, M. Ortiz-Domínguez, H. Cimenoglu, R. Escobar-Galindo, M. Keddad, M. Elias-Espinosa, N. López-Perrusquia, Surf. Eng., 27 (2011) 189-195
- [13] Z. Nait Abdellah, M. Keddad, R. Chegroune, B. Bouarour, H. Lillia, A. Elias, Matériaux et Techniques, 100 (2012) 581-588.
- [14] Z. Nait Abdellah, M. Keddad, A. Elias, Int. J. Mater. Res., 104 (2013) 260-265.
- [15] M. Kulka N. Makuch, A. Pertek, L. Maldzinski., J. Solid State Chem., 199 (2013) 196-203.
- [16] C.M. Brakman, A.W.J. Gommers, E.J. Mittemeijer, J. Mater. Res., 4 (1989) 1354-1370.
- [17] L.G. Yu, X.J. Chen, K.A. Khor, G. Sundararajan, Acta Mater., 53 (2005) 2361-2368.
- [18] H. Okamoto, J. Phase Equilib. Diffus. 25 (3) (2004) 297-298.
- [19] Z. Nait Abdellah, R. Chegroune, M. Keddad, B. Bouarour, L. Haddour, A. Elias, Defect Diffus. Forum, 322 (2012) 1-9.
- [20] V.I. Dybkov. Reaction Diffusion and Solid State Chemical Kinetics, Switzerland-UK-USA: Trans Tech Publications; 2010, p. 7.
- [21] W.H. Press, B.P. Flanery, S.A. Teukolsky, Numerical Recipes in Pascal: the Art of Scientific Computing, Cambridge University, 1989.
- [22] H. Kunst, O. Schaaber, Härterei-Tech. Mitt., 22 (1967)

- 275.
- [23] I. Campos-Silva, D. Bravo-Bárceñas, A. Meneses-Amador, M. Ortiz-Domínguez, H. Cimenoglu, U. Figueroa-López, R. Tadeo-Rosas, *Surf. Coat. Technol.* 237 (2013) 402-414.
  - [24] I. Campos-Silva, M. Ortiz-Domínguez, O. Bravo-Bárceñas, M. A. Doñu-Ruiz, D. Bravo-Bárceñas, C. Tapia-Quintero and M. Y. Jiménez-Reyes, *Surf. Coat. Technol.* 205 (2010) 403-412.
  - [25] A. Kaouka, O. Allaoui, M. Keddad, Growth kinetics of the boride layers formed on SAE 1035 steel, *Matériaux et Techniques*, 101, 705 (2013).
  - [26] K. Matiasovsky, M. Chrenkova-Paucirova, P. Fellner, M. Makyta, *Surf. Coat. Technol.* 35 (1988) 133-149.
  - [27] G. Kartal, O.L. Eryilmaz, G. Krumdick, A. Erdemir, S. Timur, *Appl. Surf. Sci.*, 257 (2011) 6928-6934.
  - [28] L.G. Yu, K. A. Khor, G. Sundararajan, *Surf. Coat. Technol.*, 157 (2002) 226-230.
  - [29] M. Ortiz-Domínguez, I. Campos-Silva, G. Ares de Parga, J. Martínez-Trinidad, M. Y. Jiménez-Reyes, G. Rodríguez-Castro, E. Hernández-Sánchez, *Kovove Mater.* 50 (2012) 115-123.
  - [30] I. Campos, G. Ramírez, U. Figueroa, J. Martínez, O. Morales, *Appl. Surf. Sci.* 253 (2007) 3469-3475.